

LASER INTERFEROMETER GRAVITATIONAL WAVE OBSERVATORY
-LIGO-
CALIFORNIA INSTITUTE OF TECHNOLOGY
MASSACHUSETTS INSTITUTE OF TECHNOLOGY

Technical Note LIGO-T000058- 00- R 5/11/2000

**Measurement of Seismic Motion at 40m
and transfer function of seismic stacks**

D. Ugolini, S. Vass, A. Weinstein

This is an internal working note
of the LIGO Project.

California Institute of Technology
LIGO Project - MS 18-34
Pasadena CA 91125
Phone (626) 395-2129
Fax (626) 304-9834
E-mail: info@ligo.caltech.edu

Massachusetts Institute of Technology
LIGO Project - MS NW17-161
Cambridge, MA 02139
Phone (617) 253-4824
Fax (617) 253-4824
E-mail: info@ligo.mit.edu

WWW: <http://www.ligo.caltech.edu/>

Measurement of Seismic Motion at 40m and transfer function of seismic stacks

Abstract

In preparation for upgrading the Caltech 40m interferometer for prototyping LIGO II optical configurations, we are measuring the seismic motion of the 40m laboratory and the transfer function of the existing seismic stacks.

1 Introduction

We are attempting to measure the seismic noise and stack transfer functions at the 40m lab. Why?

- Well, just to understand it; learn how to do it, and compare with past measurements [1].
- To evaluate the need for active isolators (STACIS, IDE; we currently think it's a good idea).
- To validate our crude modelling of the stack transfer functions, in order to estimate what they'd be if we replaced the viton with damped metal springs (which we currently think is not advisable).

Guided by the work reported in [2], We pursue two approaches:

- Use natural ground seismic motion, measure it on the floor and on top of a stack with seismometers, accelerometers, geophones, *etc.*, reading out these instruments with the DAQS system, and analyzing the resulting frames with matlab.
- Use a shaker on the floor or on the stack support bars, and a spectrum analyzer in swept-sine mode to measure the transfer functions.

2 Measurements using natural ground seismic motion

Our equipment:

- We have obtained two 3-axis geophones from MIT (Barry Controls Triaxial Microvelocity Sensor). One is typically placed on the floor (in the frames, these signals are called "Floor-X", "Floor-Y", "Floor-Z"), and the other moves around (no matter where it is placed, in the frames, these signals are called "Stack-X", "Stack-Y", "Stack-Z").

- We have a 1-axis seismometer in the lab (in the frames, “IFO-Seis”), which we can orient any way we want.
- We have a small audio microphone (in the frames, “Microphone”).

These 8 signals are routed to 8 “spare” fast (16384 Hz) channels in the existing DAQ system, and can be logged to the 40m RAID array when we want to take measurements.

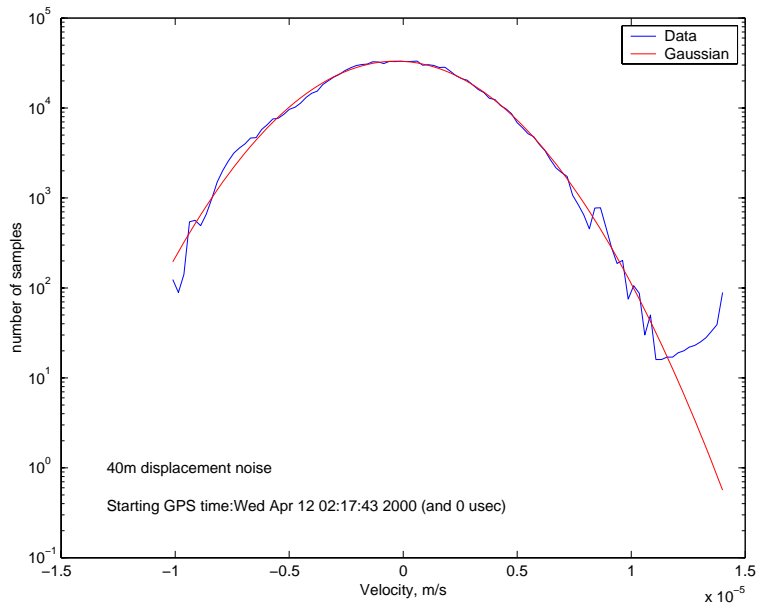
The data are transferred by ftp to a big disk on canopus (a cpu server on the general ligo.caltech.edu sun cluster) and are analyzed with matlab. We know of no way to run matlab on the 40m sun that has the raid array (cdssol9 - albireo) or to mount the raid array on the general ligo.caltech.edu sun cluster.

Calibration: The placard by the seismometer says 340 V/m/s, X20 for the preamplifier gain, for a total of 6800 V/(m/s). The geophone x- and y- coordinates are set to 1000 V/(in/sec) = 39400 V/(m/s). The geophone z-coordinates are set to 100 V/(in/sec) = 3940 V/(m/s). The VME fast ADC (a VMIC3123 16ch, 16-bit, 100kHz S/H ADC running at 16384 Hz) is set to 16384 adc counts / volt. So the final calibration constants are

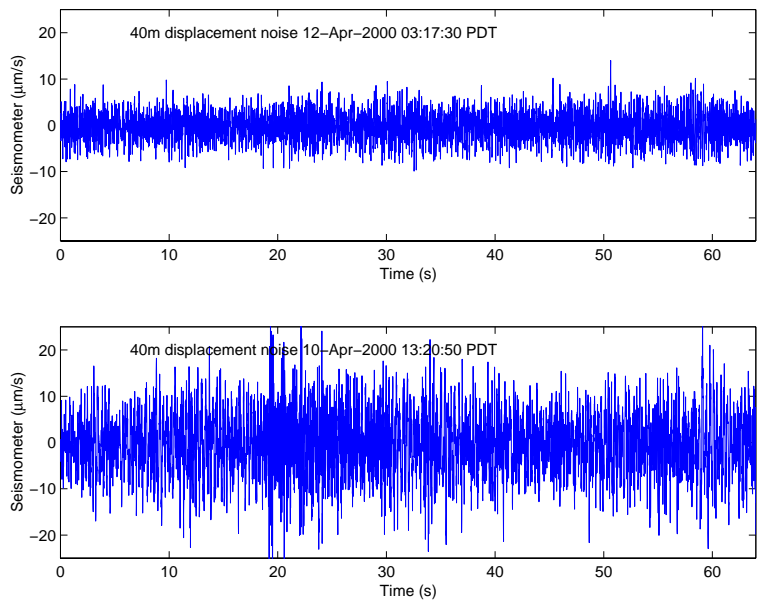
- IFO-Seis: 1 ADC count = 9.0×10^{-9} m/s
- Geophone x,y: 1 ADC count = 1.6×10^{-9} m/s
- Geophone z: 1 ADC count = 1.6×10^{-8} m/s
- The microphone is in “arbitrary units”...

2.1 Analysis

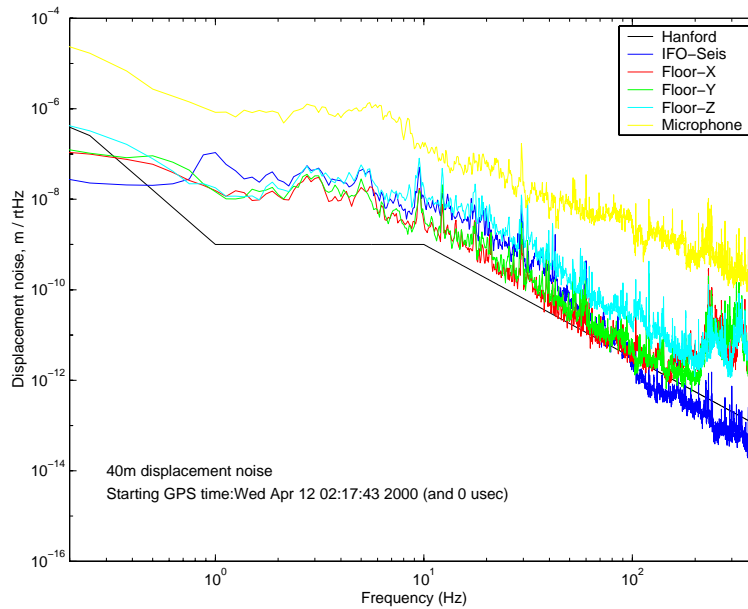
- Read in to matlab, 64 seconds of data from all 8 channels, using `frextract`, a matlab function to read frame data (from Benoit Mours’ `frame` library, but only in version 3.71, for some reason). We had to modify `frextract` to close the frame file.
- Apply calibration constants to the time series.
- Plot the seismometer time series; look for bumps to see if this is a quiet time.
- Histogram the seismometer time series, and compare with a gaussian with the same mean and σ , to look for non-gaussian seismic noise. Here’s an example from the wee hours of the night:



Note that data taken during the day are FAR less gaussian, and have peaks at $\sim 10^{-5}$ m/s. Here are two seismometer time series, one from the day and one at night:

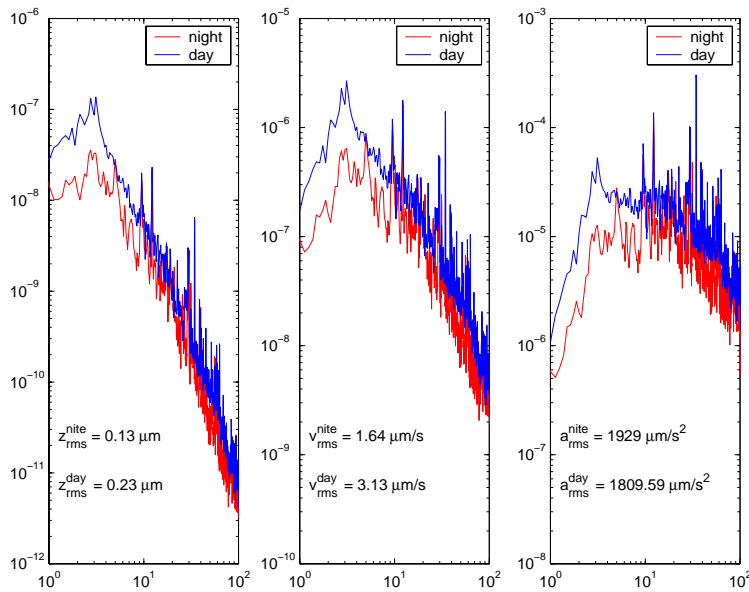


- Take an averaged power spectrum (`pwravg` code courtesy of Gabriela): subtract the mean, apply Hanning window, take fft, normalize power spectrum correctly, average 8 sets of 8 consecutive one-second intervals with no overlap.
- Convert from velocity power spectrum to displacement amplitude spectrum, by taking the square root and dividing by $2\pi f$. Here's the result, also from the wee hours, compared with the “noisy Hanford” parameterized spectrum:



Things to note:

- The seismometer reading compares well with the geophone Z axis.
- The geophone X and Y compare well, and the seismic noise appears to be roughly isotropic.
- The microphone signal has arbitrary units.
- There are spurious resonances in the geophones above 200 Hz, making them useless there.
- The geophones fall off nicely from below 10 Hz to above 100 Hz
- It's not clear why the seismometer reading falls off at 100Hz, since we think the bandpass filter is set to 0.1 – 300 Hz.
- Spectra taken during the day are noisier, but have similar features. Here we compare two spectra taken during the day and at night:



- The spectra are predictably noisier than the “noisy Hanford” parameterized spectrum.
- I have dug up the following plot from the LIGO proposal [1]. Curve B (the 40m lab) compares well with the geophone measurements, including the features at 8 Hz and 22 Hz!

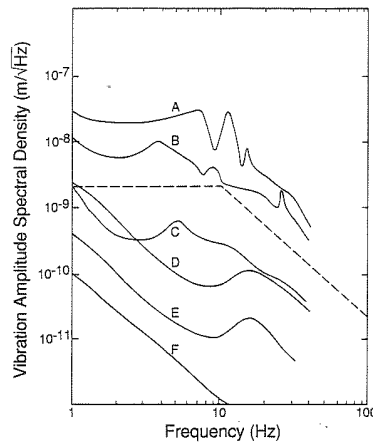
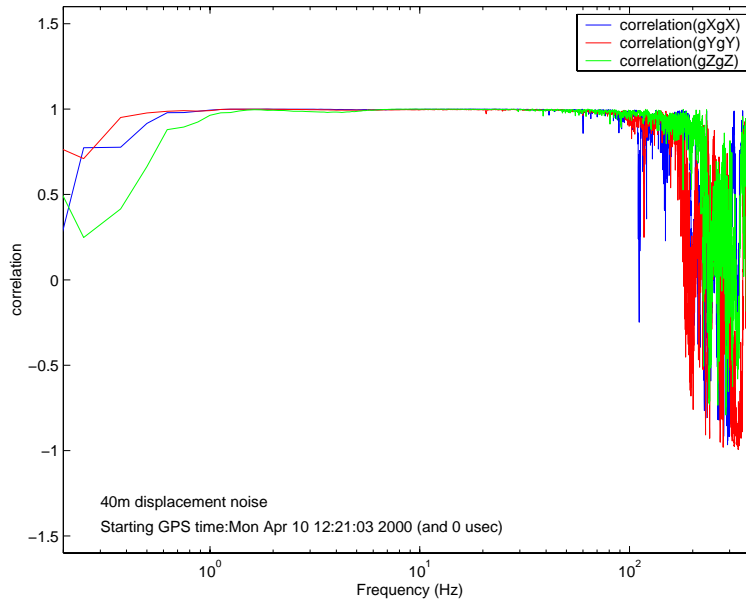


Figure II-3 Vibration amplitude spectral density data for typical motion of the ground at several locations: (A) MIT laboratory; (B) Caltech laboratory; (C and D) potential LIGO sites; (E) Lajitas, Texas (seismically quietest known location in the United States), with 3-10 mph wind conditions; (F) Lajitas, with no wind. The dashed line is the adopted LIGO specification for vibration measured at the instrument mounting structures.

- Calculate the correlation between the different channels (`freqresp` code courtesy of Gabriela): Calculate the average cross spectrum $S_{XY}(f) = \tilde{X}^*(f)\tilde{Y}(f)$ (appropriately normalized); the correlation is $Re(S_{XY})/(|\tilde{X}||\tilde{Y}|)$, and the coherence is $|S_{XY}|^2/(|\tilde{X}|^2|\tilde{Y}|^2)$.

Here’s the result when the geophones are aligned and sitting right next to each other on the floor:

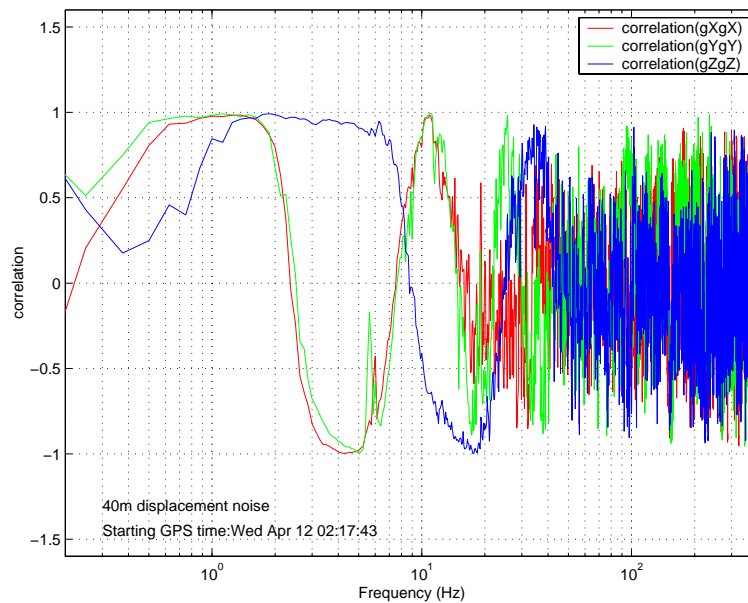
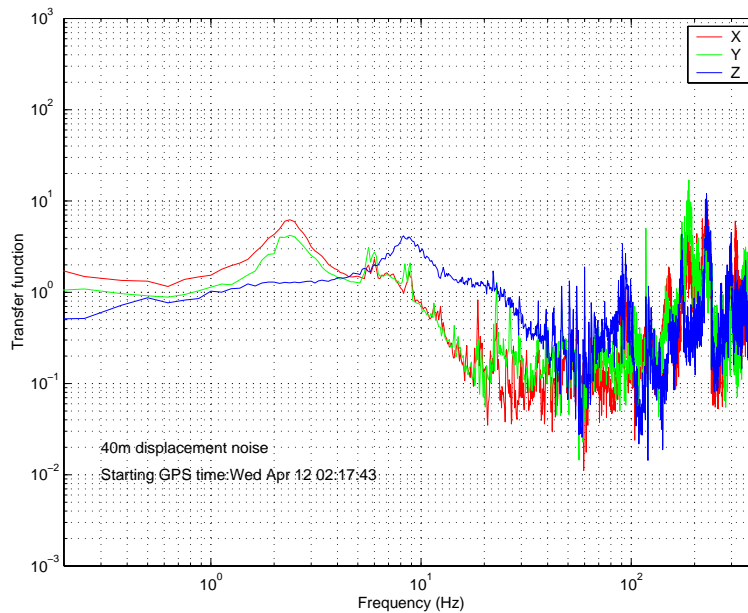


Things to note:

- The fall-off in correlations at ~ 200 Hz, and the (hard to see, but there) anti-correlation at ~ 300 Hz, corresponds to a seismic wavelength of $\lambda_s = v/f = (450 \text{ m/s})/(300 \text{ Hz}) = 1.5 \text{ m}$ or a half-wavelength of 0.75 m , roughly the separation between the geophones.
 - There are no evident correlations between other channels, eg, X and Y of the same or different geophones.
 - There are weak correlations between the seismometer and the geophone (along the axis which coincides with the seismometer orientation) in the frequency range.
- Divide the displacement power spectrum of the “Stack” geophone by that for the “Floor” geophone, to get the stack transfer function. (Or, take the amplitude of the frequency response of Stack to Floor, $S_{XY}(f)/|\tilde{X}|^2$).

When we do this for the case of both geophones on the floor, the transfer functions are consistent with 1 up to 100 Hz, above which they are dominated by noise.

When we take data with one geophone on top of the EV stack, we get the following plots of the transfer function and the correlations:



Things to note:

- The resonant peaks are clearly evident. The Z (vertical) peaks at ~ 8.5 Hz, 25 Hz, and 45 Hz are evident as peaks in the transfer function and zero-crossings in the correlation plot. Similarly, for the X and Y resonances at ~ 2.3 Hz, 7.5 Hz, 15 Hz, 22 Hz.
- From Joe Giaime's thesis [7], we know that a 3D FEA model predicts that the horizontal modes have resonant frequencies significantly lower than the vertical ones (see figure below).
- The Z (vertical) peaks are to be compared to my crude model (in which I GUESS at masses and numbers of springs) of 12.0 and 28.9 Hz, 42 Hz, and 61 Hz.
- There appears to be a fall-off from 8 - 12 Hz in the X and Y, but above that, we're not sure what's going on. We're looking to see the sharp $1/f^8$ fall-off between 40-200 Hz.

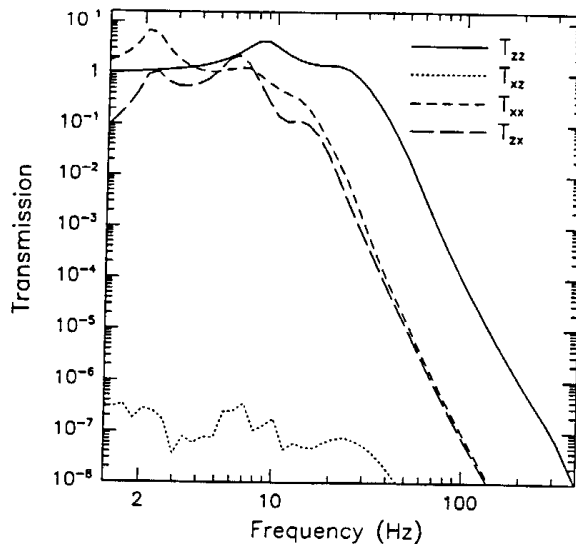


Figure 1: Transfer functions as modelled by symmetric ABAQUS model, of a viton stack similar to the 40m. From [7].

3 Transfer functions with the HP spectrum analyzer

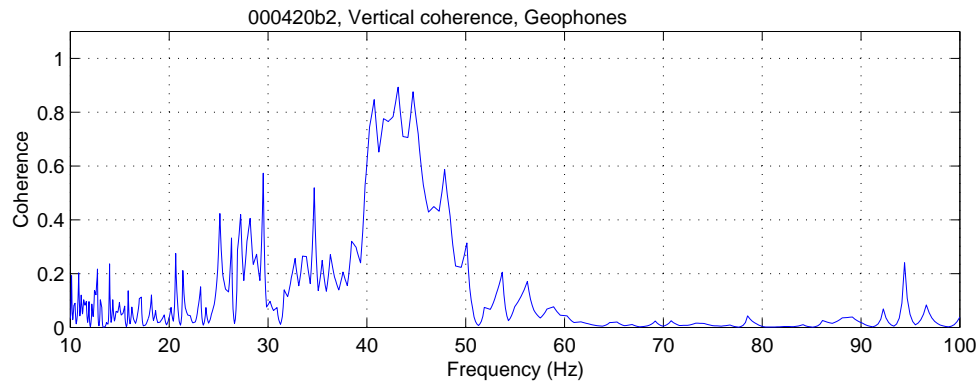
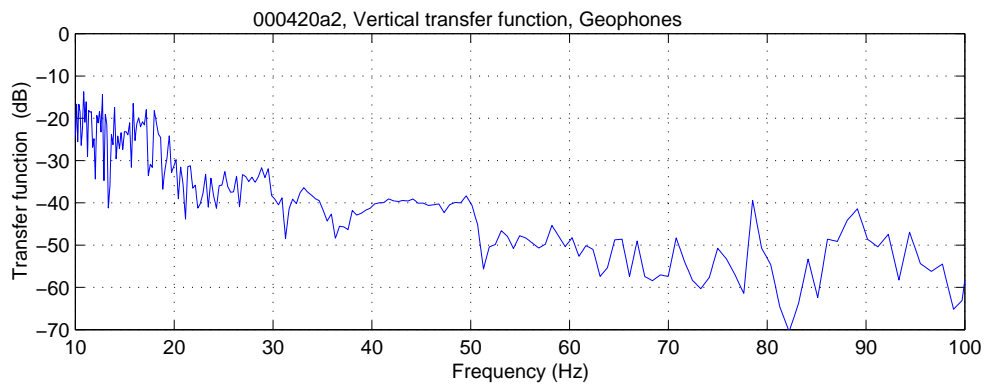
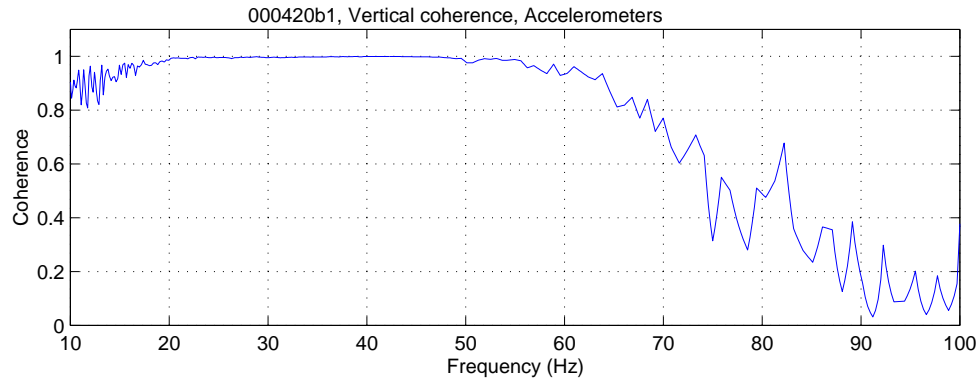
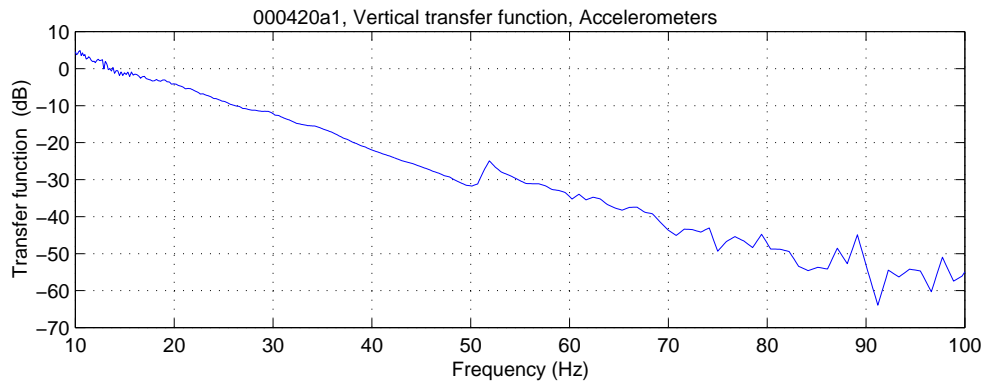
We employ the HP 3563A Control Systems Analyzer in swept sine, linear sweep measurement mode. The Source output is fed into the power amplifier of a shaker (Bruel & Kjaer Vibration Exciter Type 4809, 45 newton force rating), which is tightly clamped to the stack support beam. For measurement of the vertical transfer function, the shaker sits on the floor. For measurement of the horizontal transfer function, the shaker is butted up against a heavy object.

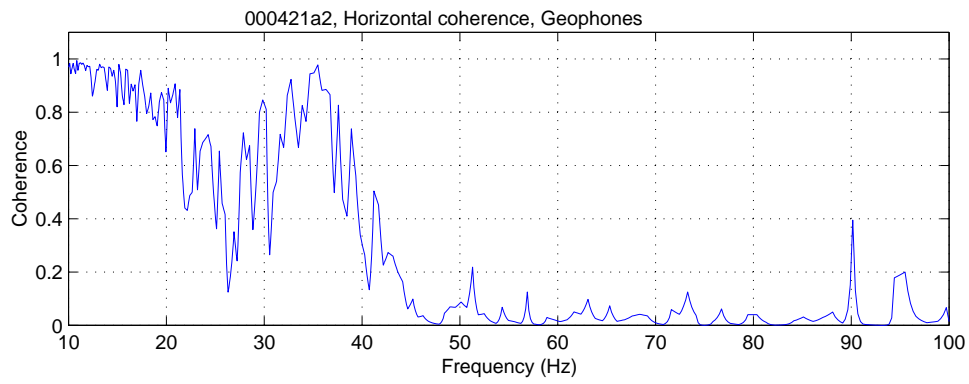
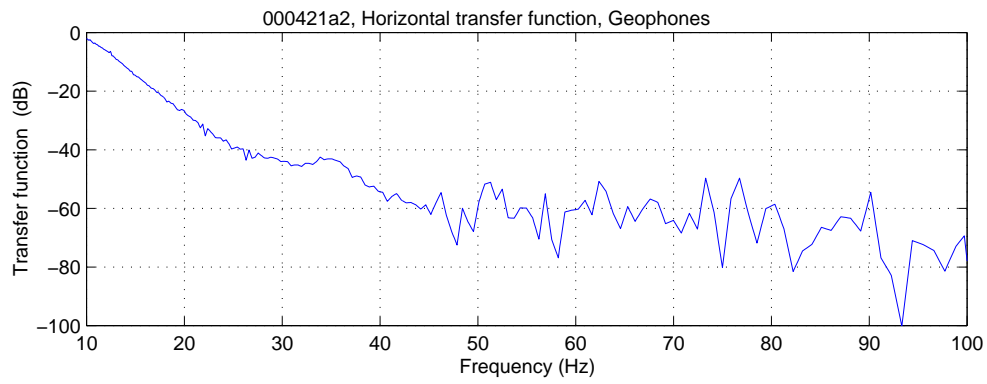
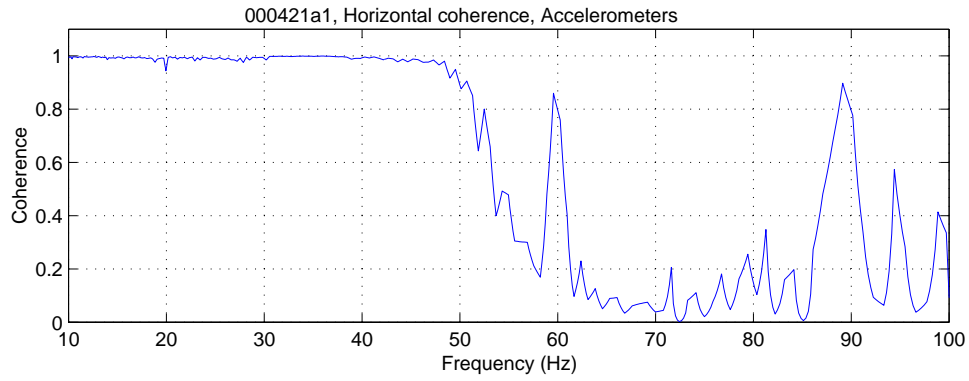
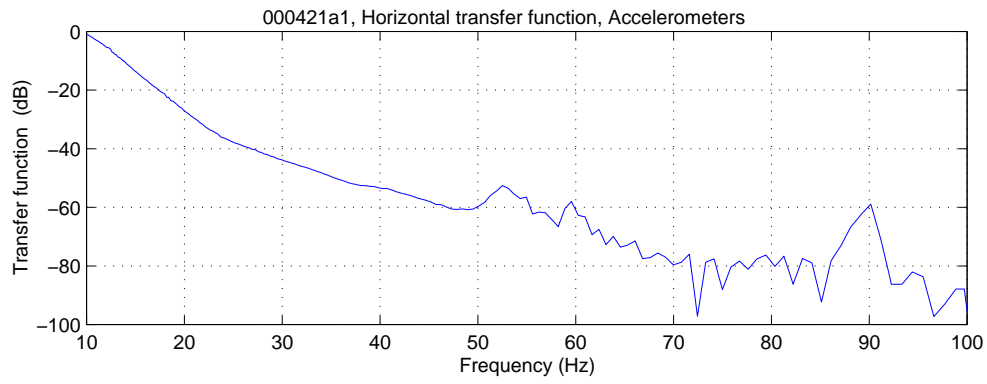
A pair of accelerometers (Bruel & Kjaer High Sensitivity Line-drive Accelerometer Type 8318) or geophones (Barry Controls Triaxial Microvelocity Sensor) is used to measure the transfer function. One rests on the stack support beam, close to the shaker, and the other rests on the top of the seismic stack. The door is closed to minimize air currents, but the system was *not* under vacuum, so acoustic noise is a big problem here.

The Spectrum Analyzer measured the frequency response and coherence, in the range from 10 to 100 Hz, in 800 linear steps, with 4 averages per step. Below 10 Hz, the shaker did not have enough oomph to produce a measurable response on the accelerometer placed next to it; above 100 Hz, there was no coherence in any of the configurations. It took about 5 minutes to complete a measurement.

The results for horizontal and vertical transfer functions, from the accelerometers and geophones, are shown in the following plots.

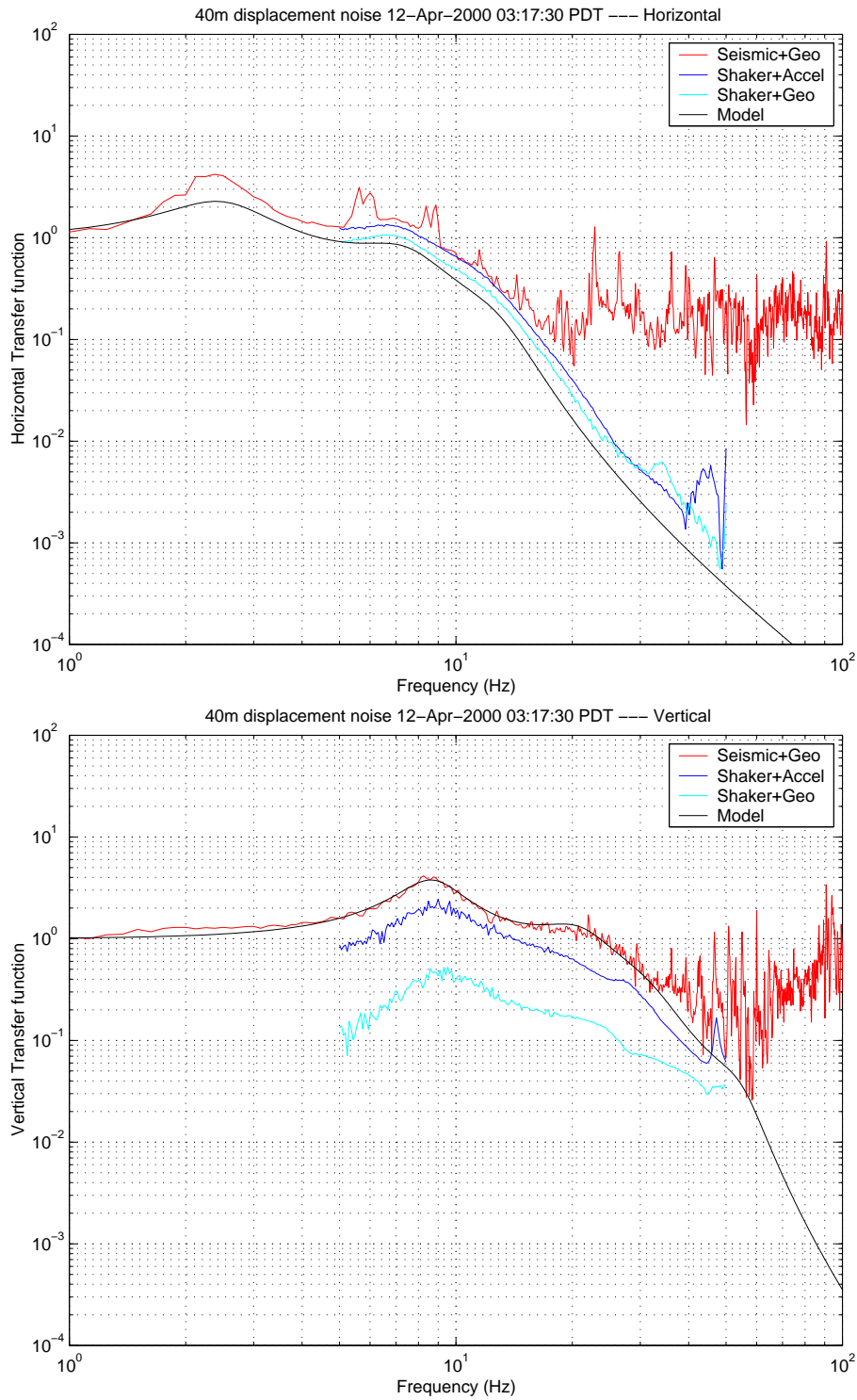
The accelerometers register nothing in response to natural ground motion, but give coherent and sensible results when used with the shaker. The geophones are pretty much useless with the shaker, even in the range (< 40 Hz) where they appear to give reliable data using natural ground motion. Perhaps the shaker is too strong for the geophones.





3.1 Comparisons

We compare the shaker measurements using the accelerometers with the geophone measurements using natural ground motion, and with model calculations incorporating an “eyeball” fit to the observed resonance frequencies, in the following figures:



Things to note:

- The measured horizontal transfer functions compare well; in the range of overlap (between 10 and 20 Hz), the shape of the transfer functions agree, and the levels agree to better than a factor 2...
- The vertical transfer functions agree in shape from 5 to 50 Hz, but the transfer function taken with the shaker and accelerometers is a factor 2 below the transfer function taken with natural ground motion and geophones. (We measured no calibration offset between the geophones when they were placed next to each other). The one taken with the shaker and geophones is lower still. This is not understood.
- The model of the vertical transfer function agrees well with the measurements made with geophones and natural seismic motion, from 1 Hz to 50 Hz. It should fall like f^{-8} above 100 Hz, but we don't know how to measure it there (without the interferometer).
- The model of the horizontal transfer function lies as much as a factor 2 below the data, but the shape agrees in the range between 5 and 40 Hz.
- The model of the vertical transfer function has 4 poles, at 8.7, 21.0, 32.0, 55.0 Hz. The model of the horizontal transfer function has 3 poles, at 2.5, 7.5, 13 Hz. Again, the models are just an eyeballing of the curves.

4 The currently existing stacks

At present, the 40m lab contains five seismic stacks with three legs and four stages, for the chambers housing the beam splitter (BS), south vertex (SV) test mass, south end (SE), east vertex (EV), and east end (EE). There is also an input optics chamber with a square optical table sitting on a one-leg, four stage stack. The layout can be seen in [3].

The three-legged stacks were installed in 4/93. The input optics chamber stack was built in 1996, and installed at the end of that year[4] Engineering drawings for these stacks exist [5].

In each of these stacks, the masses are machined stainless steel, and the springs are viton elastomer.

4.1 The transfer function

To quantify these issues at some level, we have made simple Matlab models of the vertical transfer function

$$T_{zz}(f) = \frac{x_{top}(f)}{x_{floor}(f)}$$

for stacks consisting of all viton springs, all damped metal springs, and mixtures of springs. Folding these in with the ground motion spectrum $z_{floor}(f)$ allows us to predict the spectrum of motion at the top of the stack, $z_{top}(f)$, and calculate the integrated rms motion x_{rms} and $v_{z,rms}$.

4.2 T_{zz} versus T_{xz} and T_{xx}

For IFO locking and noise performance, the relevant motion is in the direction along the beam (x). However, the stacks are arranged vertically in the local gravitational field, and it is therefore easiest to model the vertical transfer function. The more relevant T_{zx} and T_{xx} transfer functions can only be reliably estimated using 3D finite element analysis tools, which take into account the more complex couplings of z to x , and all the complex properties of all the materials, their shear moduli and geometry, etc.

Fortunately, much work has already been done in this area, by Joe Giaime and others [7]. As summarized in Fig. 1, we see that:

- T_{xz} and T_{xx} have seismic walls at frequencies typically a factor of 2 or more smaller than T_{zz} ;
- If T_{zz} has a peak at 9 Hz, T_{xz} and T_{xx} peak in the 2 to 3 Hz region, and otherwise lie below T_{zz} .
- These predictions were confirmed (qualitatively) with measurements of a test stack at MIT [7].

This figure can be used to qualitatively extrapolate from a model of T_{zz} to the more relevant T_{xz} and T_{xx} .

4.3 The modelled transfer function

The stacks are designed and modelled as described in the appendix. Here we focus only on the three-legged stacks housing the core optical components; the input and output chamber stacks have similar properties and less critical requirements.

The vertical transfer function T_{zz} is shown in Fig. 2, and the vertical motion at the top of the stack, $z_{top}(f)$, is shown in Fig. 3. In both figures, we show the stacks with all viton springs, all damped metal springs, and a mixture.

The features to note are:

- At high frequencies, all the stack transfer functions have the expected f^{-8} falloff.
- The metal stacks have superior isolation at higher frequencies compared with the viton, with the mixed stacks lying in between. The frequency at which the vertical displacement falls below 1^{-18} m/ $\sqrt{\text{Hz}}$ is 39 Hz for metal and 91 Hz for viton.
- The metal stacks have resonant peaks that are less damped and at lower frequencies than the viton stacks, leading to higher peak motion at the resonant frequencies. The viton peaks are all but washed out by the damping.

The numbers used for the springs, all of which probably require confirmation, are summarized in table 1.

The numbers for the stacks are summarized in table 2. Analogous tables for LIGO stacks appear in Ref. [6], and we have checked our calculations against all the numbers in those tables.

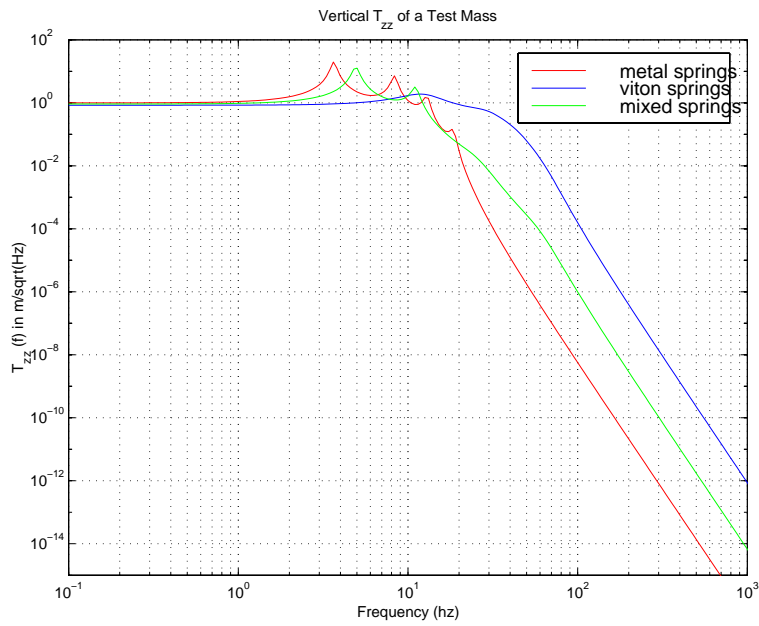


Figure 2: Vertical transfer function T_{zz} (predicted) for 40m seismic stacks built with damped metal springs, viton springs, or a mixture.

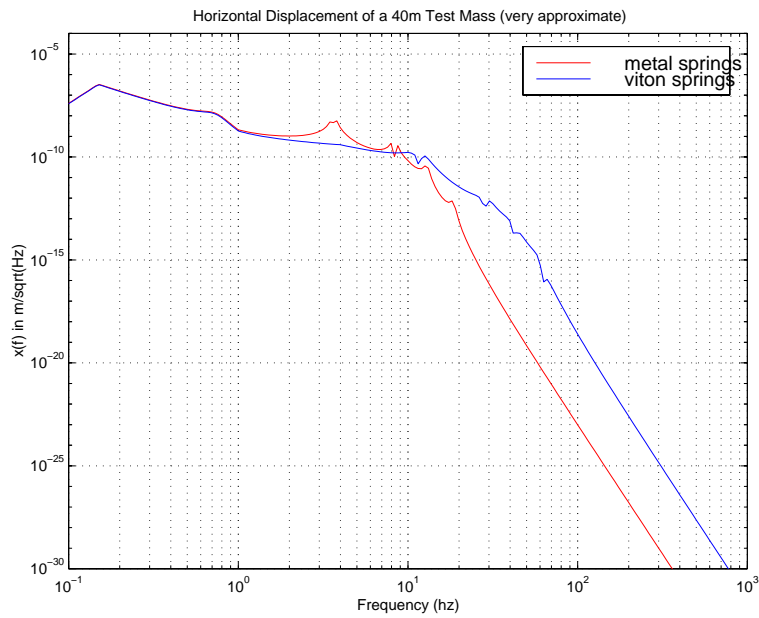


Figure 3: Vertical motion $z(f)$ (predicted) for 40m seismic stacks built with damped metal springs, viton springs, or a mixture.

Table 1: Spring parameters.

Spring:	damped metal	viton
k at 100 Hz (Nt/m)	66317	832400
P_{max} (kg)	45	57
η (%)	4	30
Q	25	3.3

Table 2: Stack parameters for 40m three-legged stacks with viton springs, according to these calculations (the reality is to be determined upon disassembly, since we can't find original specifications). The masses and cumulative masses are for the entire stage, summing all three legs. The number of springs $n_{springs}$ is fixed to an integral multiple of 3. The ratio of the actual load to the maximal load borne by the springs is P_{load}/P_{max} . The resonant frequencies of each stage, f_{stage} , is given assuming no couplings between stages, and f_{norm} is from a normal mode analysis of those couplings.

Stage	mass (kg)	cum mass (kg)	$n_{springs}$	P_{load}/P_{max} (%)	f_{stage} (Hz)	f_{norm} (Hz)
Payload	50	50				
4 (top)	173	223	6	66	24.1	12.0
3	275	498	9	98	26.5	28.9
2	275	773	15	91	34.3	42.4
1 (bot)	275	1048	21	88	40.6	60.7

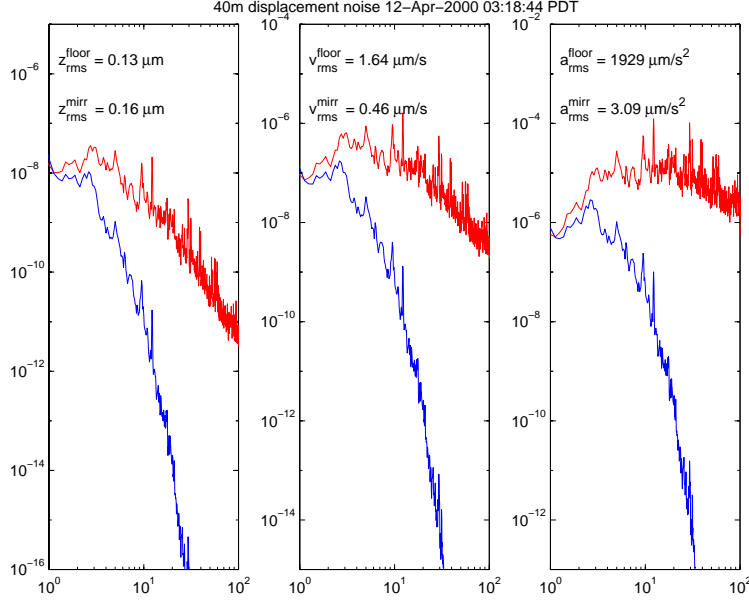
Total springs/stack = 51.
 $\log_{10}(T_{zz})$ at 100 Hz = -3.80.

5 Noise tolerance for lock acquisition

Lock acquisition depends primarily on the free-swinging velocity (distribution and rms) of the mirror, hung from the suspension pendulum resting on the seismic stack.

If we believe our model of the stack transfer function, and a simple model for a single pendulum with $f_0 = 0.74$ Hz and $Q = 3$, we can predict the velocity spectrum at the mirror.

Here we compare the horizontal displacement, velocity, and acceleration spectra measured at the floor, with the predicted spectra at the mirror, using the modelled stack and pendulum transfer functions:



Now we calculate an rms velocity for the two spectra. We verify Parseval's theorem for the velocity spectrum measured at the floor: the standard deviation of the velocity time series is equal to the rms velocity calculated from the power spectrum:

$$v_{rms}^2 = \sum (X(t_i) - \bar{X})^2 / N = \sum |\tilde{X}(f_i)|^2 \Delta f$$

OK, the rms velocity on the floor and the mirror are noted in the figure above.

These data were taken at 3am. Data taken during the daytime can yield rms velocities a factor 2 or more higher, as illustrated by a figure several pages back.

5.1 Mean time to lock

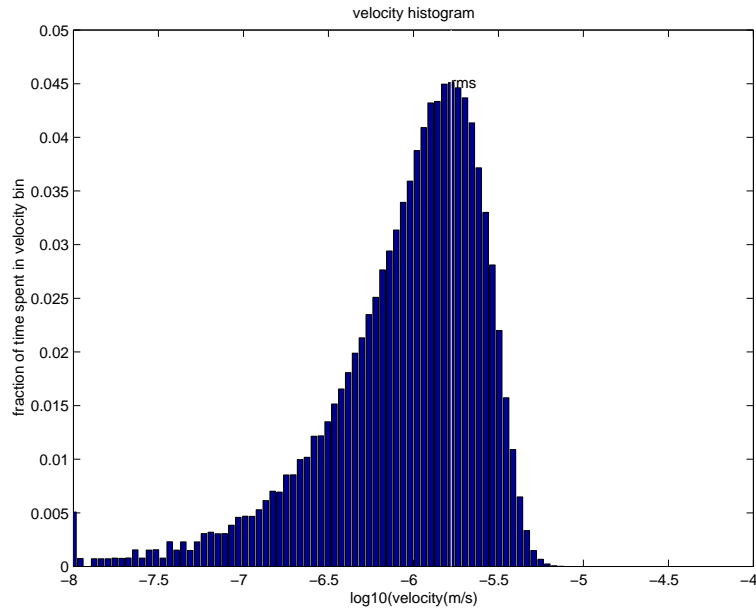
The mean time to lock [8] (MTTL) is given crudely by

$$\tau_{lock} \sim \frac{\lambda/2}{v_{thr} P(v < v_{thr})}$$

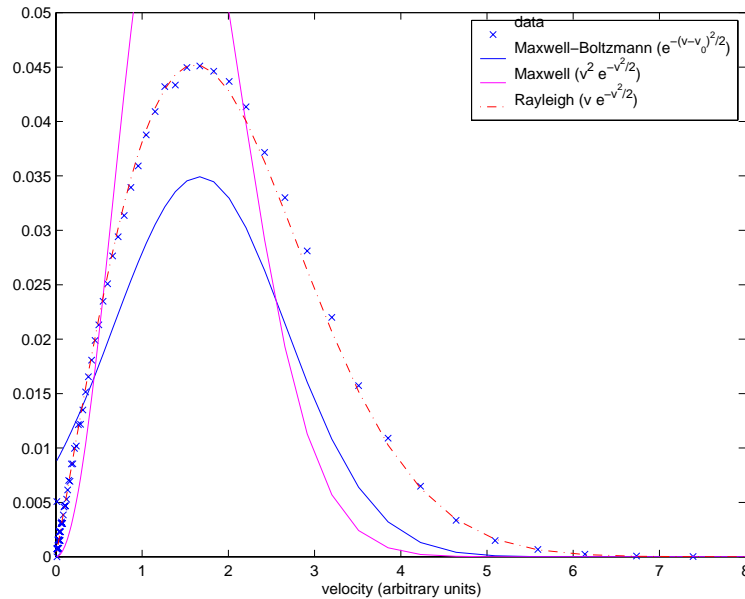
where $\lambda = 1.064 \times 10^{-6}$ m, the threshold velocity v_{thr} is the velocity mirror below which the controllers will always acquire lock, and P is the probability, given the mirror velocity distribution, that the velocity is below v_{thr} . The threshold velocity v_{thr} is a complex function of the controller loop gain and bandwidth, but for LIGO it is supposed to be around $1 \mu\text{m/s}$ or $1 \lambda/\text{s}$.

The rms velocity v_{rms} of the mirror as estimated above is on the order of $1 \mu\text{m/s}$ or $1 \lambda/\text{s}$. This compares well with The threshold velocity v_{thr} , so that the mean time to lock is expected to be of order 1s.

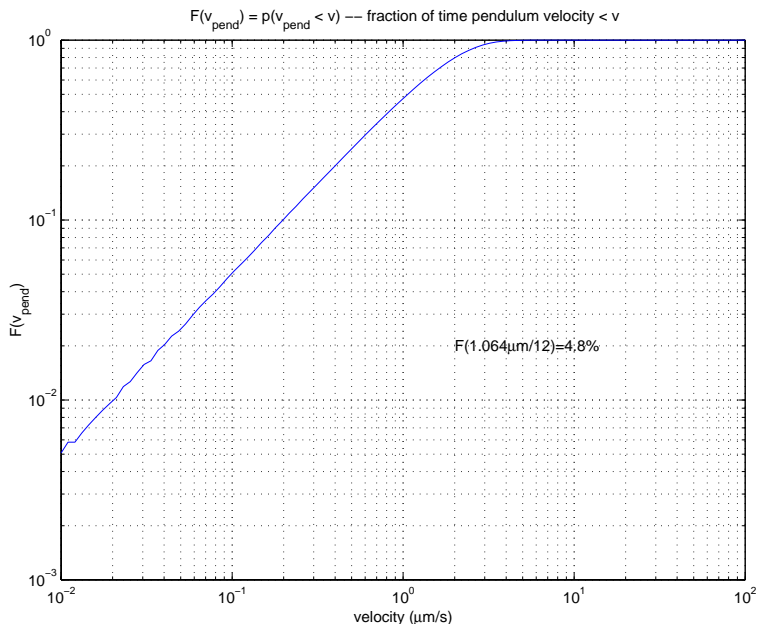
To evaluate $P(v < v_{thr})$, we make use of the matlab program `velhist.m`, developed by Gabriela Gonzalez and Brent Ware. We histogram the floor-Y velocity distribution (eventually, we'll fold in the stack and pendulum transfer functions into this calculation),



We can compare this distribution (now with a linear x-scale) with idealized curves: The Rayleigh distribution describes the data well.



Then we form the cumulative velocity distribution and determine the fraction of time $P(v_{mirr} < v)$ that the mirror velocity falls below v (the x axis).



Choosing a threshold velocity of $v_{thr} = 1/12 \lambda/s$ (as was taken in ref. [8]), we get $P(v_{mirr} < v_{thr}) = 4.8\%$, or a MTTL of 125 seconds. If instead we take $v_{thr} = 1 \lambda/s$, we get $P(v_{mirr} < v_{thr}) = 50\%$, or a MTTL of 1 second.

A reliable estimate of the MTTL depends on a reliable estimate of the threshold velocity, which in turn depends on the details of the control system (gain and bandwidth). It also depends on whether one is running during the noisy daytime or the quiet evening.

Here we can only note that the rms velocity of the mirrors is “in the ballpark” of having a MTTL on the order of seconds.

6 Active seismic isolation?

The prototyping of a control system for RSE will be challenging enough, without having to worry about seismic noise making the IFO difficult to lock. At this early stage in the upgrade, we should consider ways to suppress this, even in the absence of good quantitative guidance.

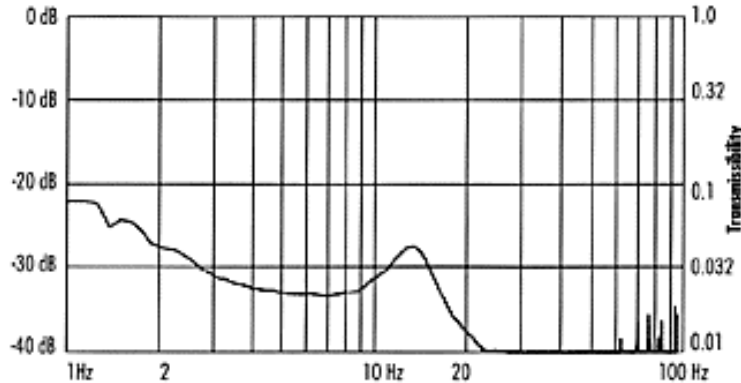
An approach that has been used at MIT’s PNI [9] was to use Barry Controls STACIS PZT-stack-based active isolation system [10]. We have been investigating this (they’re now sold by TMC [11]), and their competitors in Germany, IDE [12].

These systems are comprised of pedestals, which would sit on the floor. The seismic stack support beams, which currently connect to feet which sit on the floor, would instead have to connect to “cradles” which would rest on the pedestals. This is a rather big job, in terms of mechanical engineering:

- One must ensure that the weight of the stacks are adequately supported, and that tilts are controlled;
- no excessive forces (especially torques) can be applied to the support beams since they penetrate the vacuum chamber in rather fragile vacuum bellows
- no excessive horizontal force can be applied to the pedestals themselves, especially during an earthquake, since they are not built to withstand such forces.

These systems are expensive: a pedestal costs in the neighborhood of \$10K, and we need three for each of 4 test mass stacks, for a total of 12.

These devices rely on a rubber mat for passive vertical isolation at high frequencies, and active PZT stacks to (attempt to) keep the transfer function below 1 in the vicinity of the low-frequency resonances. They're relatively stiff systems; their resonant frequencies are in the neighborhood of 1 Hz. Here's the Horizontal Transmissibility from the STACIS-2000 web site:



Unfortunately, these figures cut off at the low end, where the pedestal resonances occur, so we don't know whether they amplify or attenuate the motion in the microseismic band.

To see the quantitative effect of adding these systems to the stacks, we need just a simple model of the vertical and horizontal transfer functions (in loop). It's hard to get reliable information on this, from the manufacturers. Some attempt at mocking it up, roughly matching the figure shown above in the 1–20 Hz band, yields a reduction in the horizontal v_{rms} by as much as a factor 2 (ie, from $v_{rms} = 0.46 \mu\text{m/s}$ to around 0.23), but different behavior below 1 Hz could wipe that out. A factor 2 in v_{rms} translates into a factor 2 in MTTL. We are attempting to get more useful information from the manufacturer.

7 Summary

We have measured the natural seismic ground noise in the 40m laboratory using geophones, during the day and late at night. It compares well with previous measurements.

We have measured the 40m BS seismic stack transfer function using two approaches: First, using natural seismic ground noise, 3-axis geophones, and the 40m DAQ system. Second, using a shaker, 1-axis accelerometers, and the HP signal analyzer. In the region of overlap, these two approaches agree in shape, but the vertical transfer function measured with the shaker is a factor of two lower; this is not understood.

We attempt crude models of the stack transfer functions; the model works well for the vertical but fails for the horizontal, above 10 Hz. This is not understood.

From the models of the stack and the simple LIGO suspension pendulum, we estimate the rms velocity of the mirror. Combining this with an estimate of the threshold velocity for the lock acquisition system (which depends on details of gains and bandwidth, and lies in the 1/12 to 1 λ/s range), we estimate the mean time to lock. This can range from a few seconds to a few minutes.

We attempt to estimate the effect of adding active seismic isolation. Modulo uncertainties in the performance of these devices, they could improve the mean time to lock by a factor 2.

Since the mean time to lock is of the order of seconds, we're "on the edge" of being able to operate reliably. It's not clear (to me) from the numbers whether active seismic isolation can make

the difference between easy and hard lock acquisition, and thus, whether it is worth the effort and expense to implement it...

8 Acknowledgements

Many thanks to Gabriela Gonzalez, Fred Raab, Joe Giaime, Riccardo DeSalvo and his group, for advice and help.

References

- [1] LIGO Proposal to the NSF, LIGO-M890001-00-M.
- [2] “Transfer function and drift measurements on the first-article HAM”, M. Barton, J. Giaime, G. Gonzalez, W. Johnson, A. Marin. LIGO-T980084-00, 10/98.
- [3] LIGO drawing D961304-06: http://www.ligo.caltech.edu/LIGO_web/dcc/docs/D961304-06.pdf .
- [4] LIGO note M960115-00, http://www.ligo.caltech.edu/LIGO_web/dcc/docs/M960115-00.pdf .
- [5] LIGO drawings 1205425-1205429, 1205431-1205433, 1205435-1205439, 1205441-1205452, 1202092, 1101012.
- [6] E. Ponslet, HYTEC-TN-LIGO-01 (1996); HYTEC-TN-LIGO-02 (1996); HYTEC-TN-LIGO-03 (1996); HYTEC-TN-LIGO-04a (1996); HYTEC-TN-LIGO-07a (1997);
- [7] J. Giaime, PhD thesis, MIT (1995); J. Giaime, P. Saha, D. Shoemaker, and L. Sievers, Rev. Sci. Instrum. 67, 208-214 (1996).
- [8] “The BIG BOOK of LIGO Lock Acquisition Design”, B. Ware, LIGO-T-980666-00-D, 8/98.
- [9] Partha Saha, Ph.D thesis, LIGO-P970012-00-R, MIT, February 1997.
- [10] “Performance of the Barry Controls, Inc STACIS active isolation system”, P. Fritschel and G. Gonzalez, LIGO-T950046-00-R, 1995.
- [11] <http://www.techmfg.com/Products/Advanced/STACIS2000.htm> .
- [12] <http://www.ideworld.com/IDE/hauptindex.html> .